Inorganic Chemistry
Article

Inorg. Chem. **2011**, *50*, 261–270 **261**
DOI: 10.1021/ic101901w

Trinuclear-based Copper(I) Pyrazolate Polymers: Effect of Trimer π-Acid···Halide/Pseudohalide Interactions on the Supramolecular Structure and Phosphorescence

Lei Hou,[#] Wen-Juan Shi,[#] Yao-Yu Wang,* Hai-Hua Wang, Lin Cui, Peng-Xiang Chen, and Qi-Zhen Shi

Key Laboratory of Synthetic and Natural Functional Molecule Chemistry of the Ministry of Education, Shaanxi Key Laboratory of Physico-Inorganic Chemistry, College of Chemistry & Materials Science, Northwest University, Xi'an 710069, P. R. China. [#] These authors contributed equally to this work.

Received September 16, 2010

Under different situations, solvothermal reactions of 3,5-diethyl-4-(4-pyridyl)-pyrazole (HL) with CuX or CuX_2 (X = Cl, Br, I, and SCN) afforded five copper(I) coordination polymers, $\{CuX[CuL]_3 \cdot solvent\}_n$ (X = Cl, **1**; Br, **2**; I, **3**; X = SCN and solvent = MeCN, **4**) and $\{Cu_2I_2[CuL]_3\}_n$ (**5**). X-ray diffraction analyses show that all the complexes have trinuclear $[CuL]_3$ (referred as $\mathbf{Cu_3}$) secondary building units featuring planar nine-membered Cu_3N_6 metallocycles with three peripheral pyridyl groups as connectors, which are further linked by CuX or Cu_2X_2 motifs to generate single- or double-strand chains. Interestingly, the Cu(I) atoms within the $\mathbf{Cu_3}$ units in **1**−**5** behave as coordinatively unsaturated π-acid centers to contact soft halide/pseudohalide X atoms of CuX and Cu_2X_2 motifs, which lead to novel sandwich substructures of $[(\mathbf{Cu_3})(Cu_2X_2)(\mathbf{Cu_3})]$ (X = Br, I, and SCN) in **2**−**4**. In addition, both the π-acid $[\mathbf{Cu_3}]\cdots$X contacts and intertrimer Cu···Cu interactions contribute to the one-dimensional (1D) double-strand and 2D/3D supramolecular structures of **1**−**5**. All of these complexes exhibit high thermostability and bright solid-state phosphorescence upon exposure to UV radiation at room temperature. The emissions arise from the mixtures of metal-centered charge transfer, metal to ligand charge transfer, and halide-to-ligand charge transfer excited states, and can be tuned by intermolecular π-acid $[\mathbf{Cu_3}]\cdots$halide/pseudohalide contacts.

Introduction

Currently, luminescent transition-metal complexes have become an active research area since they play an important role in device displays[1] and chemosensors.[2] In the research of luminescent materials, functional complexes containing monovalent Cu(I) ions with d^{10} closed-shell electronic configurations have received the most attention for their abundant resources, peculiar photoresponse, cheap cost, and nontoxic properties compared with noble metal complexes. Furthermore, owing to the diverse coordination geometries such as linear, trigonal planar, and tetrahedral modes, the Cu(I) ion, behaving as a soft Lewis acid, is an attractive candidate for the coordinatively unsaturated metal center (UMC) because the low-coordinated (two- or three-coordinated) Cu(I) center holds many unoccupied sites and is readily accessible for other Lewis bases, such as halide and pseudohalide anions. The incorporation of UMCs into a luminescent complex represents an intriguing strategy for

Scheme 1. The Synthetic Pathways to the Complexes **1**−**5** and Their Different π-Acid $[\mathbf{Cu_3}]\cdots$Halide/Pseudohalide Connectivities

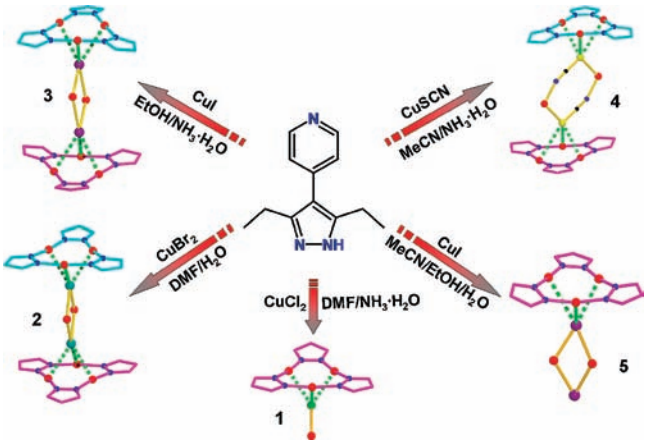

*To whom correspondence should be addressed. E-mail: wyaoyu@nwu.edu.cn (Y.-Y.W.). Tel: (86)-20-88303097.

(1) Ropp, R. C. *Luminescence and the Solid State*, 2nd ed.; Elsevier: Amsterdam, 2004.

(2) (a) Exstrom, C. L.; Sowa, J. R. J.; Daws, C. A.; Janzen, D.; Mann, K. R.; Moore, G. A.; Stewart, F. F. *Chem. Mater.* **1995**, *7*, 15. (b) Cariati, E.; Bu, X.; Ford, P. C. *Chem. Mater.* **2000**, *12*, 3385. (c) Buss, C. E.; Mann, K. R. *J. Am. Chem. Soc.* **2002**, *124*, 1031. (d) Lu, W.; Chan, M. C. W.; Zhu, N.; Che, C.-M.; He, Z.; Wong, K.-Y. *Chem.—Eur. J.* **2003**, *9*, 6155. (e) Allendorf, M. D.; Bauer, C. A.; Bhakta, R. K.; Houk, R. J. T. *Chem. Soc. Rev.* **2009**, *38*, 1330.

(3) Mao, Z.; Chao, H.-Y.; Hui, Z.; Che, C.-M.; Fu, W.-F.; Cheung, K.-K.; Zhu, N. *Chem.—Eur. J.* **2003**, *9*, 2885.

Published on Web 12/08/2010

Table 1. Crystal and Structure Refinement Data for Complexes **1**−**5**

	1	**2**	**3**	**4**	**5**
empirical formula	$C_{36}H_{42}ClCu_4N_9$	$C_{36}H_{42}BrCu_4N_9$	$C_{36}H_{42}Cu_4IN_9$	$C_{39}H_{45}Cu_4N_{11}S$	$C_{36}H_{42}Cu_5I_2N_9$
formula weight	890.40	934.86	981.85	954.08	1172.29
temp/K	295 (2)	295 (2)	295 (2)	295 (2)	295 (2)
crystal system	monoclinic	monoclinic	triclinic	monoclinic	monoclinic
space group	$P2_1/m$	$C2/m$	$P\bar{1}$	$P2_1/n$	$P2_1/n$
a/Å	7.571(2)	15.060(6)	12.0541(6)	13.8096(8)	13.0979(13)
b/Å	19.468(5)	19.446(7)	12.6890(6)	19.0144(12)	22.008(2)
c/Å	12.930(4)	14.059(8)	13.7213(7)	15.8329(10)	14.7518(14)
α/deg			107.004(1)		
β/deg	100.719(4)	112.943(4)	103.246(1)	91.090(2)	102.178(1)
γ/deg			101.501(1)		
V/Å^3	1872.6(9)	3791(3)	1871.88(16)	4156.7(4)	4156.6(7)
Z	2	4	2	4	4
D_c/g cm^{-3}	1.579	1.638	1.742	1.525	1.873
μ/mm^{-1}	2.351	3.306	3.106	2.112	4.040
F(000)	908	1888	980	1952	2288
reflns collected	10235	9849	13618	19170	20459
unique reflections	3793	3797	7260	7853	7289
R_{int}	0.0628	0.0725	0.0225	0.0482	0.0429
R_1 (all data), wR_2	0.1255, 0.1974	0.1177, 0.1759	0.0527, 0.1036	0.1260, 0.1760	0.0759, 0.1341
$R_1{}^{\alpha}$ [$I > 2\sigma(I)$], $wR_2{}^{\alpha}$	0.0624, 0.1587	0.0610, 0.1533	0.0393, 0.0936	0.0560, 0.1345	0.0473, 0.1173
GOF	1.027	1.049	1.021	1.009	1.085

$^{\alpha}\ R_1 = \Sigma(|F_o| - |F_c|)\ /\Sigma|F_o|$; $wR_2 = [\Sigma w(F_o^2 - F_c^2)^2/\Sigma w(F_o^2)^2]^{1/2}$.

luminescence modification[3] because UMCs can strongly interact with solvent molecules and anions, as well as be involved in metallophilic interactions,[4] which have great effect on the luminescence of the complex. However, it is challenging to restrict the coordination number of Cu(I) ion by using common ligands, owing to the preference of Cu(I) ion for a tetrahedral rather than a linear or trigonal planar coordination geometry. Conversely, Cu(I) ions tend to coordinate linearly in the presence of exobidentate pyrazolate (pz) ligands and form cyclic trinuclear $[Cu(pz)]_3$ complexes.[5]

The cyclic trinuclear coinage-metal (i.e., Cu(I), Ag(I), Au(I)) pyrazolate complexes $[M(pz)]_3$ (referred as $\mathbf{M_3}$), featuring nine-membered M_3N_6 metallocycles with linear two-coordinated M(I) sites as UMCs, are of significant interest because of their structural diversity,[6] fascinating luminescent properties,[7] and tendency to form supramolecular aggregates through metallophilic interactions.[8] Interestingly, the $\mathbf{M_3}$ units can behave as π-acid motifs and interact with electron-rich arenes.[9] As a result, some trimers exhibit bright luminescence, moreover, which can be fine- and coarse-turned to multiple bright visible colors by varying π-acid/base guest molecules, solvents, concentration, temperatures, and excitation wavelengths.[7,9a,10−12] Nevertheless, luminescent coordination polymers based on $\mathbf{M_3}$ units remain scarcely reported.[4a,13]

To construct a polymeric structure based on $\mathbf{M_3}$ unit, a tridentate or tetradentate functionalized pyrazolate ligand is necessary. Since the coinage metals and 3,5-disubstituted pyrazolates are frequently assembled as neutral $[M(pz)]_3$ trimers,[5,6,10,11,14] 3,5-diethyl-4-(4-pyridyl)pyrazole (HL), a potentially tridentate ligand is chosen in this presentation, which combines the coordination features of pyrazole and pyridyl ligands. The former is expected to form cyclic trinuclear units with linear coordinated coinage metals (Scheme 1), while the latter extends trinuclear units by bridging a second metal center into a coordination polymer. On the other hand, halide and pseudohalide anions are employed as soft Lewis bases, besides balancing the charges of the structures, which can be anticipated to interact with coordinatively unsaturated metals of the π-acid $\mathbf{M_3}$ units, and thus further influence structural self-assembly and luminescent properties. Sparked by this strategy, five coordination polymers $\{CuX[CuL]_3\cdot$ solvent$\}_n$ (X = Cl, **1**; Br, **2**; I, **3**; X = SCN and solvent = MeCN, **4**) and $\{Cu_2I_2[CuL]_3\}_n$ (**5**) based on $[CuL]_3$ (referenced as $\mathbf{Cu_3}$) units have been obtained, which exhibit the Cu···X interactions between π-acid $\mathbf{Cu_3}$ units and CuX or Cu_2X_2 motifs. Herein, we describe the syntheses, characterizations,

(4) (a) Zhang, J.-P.; Kitagawa, S. *J. Am. Chem. Soc.* **2008**, *130*, 907. (b) Fan, J.; Zhu, H.-F.; Okamura, T.; Sun, W.-Y.; Tang, W.-X.; Ueyama, N. *Chem.—Eur. J.* **2003**, *9*, 4724. (c) Serykh, A. I.; Kazansky, V. B. *Phys. Chem. Chem. Phys.* **2004**, *6*, 5250. (d) Serykh, A. I.; Amiridis, M. D. *Microporous Mesoporous Mater.* **2006**, *94*, 320. (e) Hao, H.-Q.; Liu, W.-T.; Tan, W.; Lin, Z.-J.; Tong, M.-L. *Cryst. Growth Des.* **2009**, *9*, 457. (f) Liu, C.-S.; Chen, P.-Q.; Yang, E.-C.; Tian, J.-L.; Bu, X.-H.; Li, Z.-M.; Sun, H.-W.; Lin, Z.-Y. *Inorg. Chem.* **2006**, *45*, 5812.

(5) (a) Ehlert, M. K.; Rettig, S. J.; Storr, A.; Thompson, R. C.; Trotter, J. *Can. J. Chem.* **1990**, *68*, 1444. (b) Dias, H. V. R.; Polach, S. A.; Wang, Z. *J. Fluor. Chem.* **2000**, *103*, 163. (c) Ardizzoia, G. A.; Cenini, S.; La Monica, G.; Masciocchi, N.; Maspero, A.; Moret, M. *Inorg. Chem.* **1998**, *37*, 4284. (d) Ehlert, M. K.; Rettig, S. J.; Storr, A.; Thompson, R. C.; Trotter, J. *Can. J. Chem.* **1992**, *70*, 2161. (e) Fujisawa, K.; Ishikawa, Y.; Miyashita, Y.; Okamoto, K.-i. *Chem. Lett.* **2004**, *33*, 66. (f) Raptis, R. G.; Fackler, J. P., Jr. *Inorg. Chem.* **1988**, *27*, 4179.

(6) La Monica, G.; Ardizzoia, G. A. *Prog. Inorg. Chem.* **1997**, *46*, 151.

(7) (a) Enomoto, M.; Kishimura, A.; Aida, T. *J. Am. Chem. Soc.* **2001**, *123*, 5608. (b) Dias, H. V. R.; Diyabalanage, H. V. K.; Rawashdeh-Omary, M. A.; Franzman, M. A.; Omary, M. A. *J. Am. Chem. Soc.* **2003**, *125*, 12072.

(8) (a) Singh, K.; Long, J. R.; Stavropoulos, P. *J. Am. Chem. Soc.* **1997**, *119*, 2942. (b) Singh, K.; Long, J. R.; Stavropoulos, P. *Inorg. Chem.* **1998**, *37*, 1073.

(9) (a) Omary, M. A.; Elbjeirami, O.; Gamage, C. S. P.; Sherman, K. M.; Dias, H. V. R. *Inorg. Chem.* **2009**, *48*, 1784. (b) Dias, H. V. R.; Gamage, C. S. P. *Angew. Chem., Int. Ed.* **2007**, *46*, 2192.

(10) Dias, H. V. R.; Diyabalanage, H. V. K.; Eldabaja, M. G.; Elbjeirami, O.; Rawashdeh-Omary, M. A.; Omary, M. A. *J. Am. Chem. Soc.* **2005**, *127*, 7489.

(11) Omary, M. A.; Rawashdeh-Omary, M. A.; Gonser, M. W. A.; Elbjeirami, O.; Grimes, T.; Cundari, T. R.; Diyabalanage, H. V. K.; Gamage, C. S. P.; Dias, H. V. R. *Inorg. Chem.* **2005**, *44*, 8200.

(12) Tekarli, S. M.; Cundari, T. R.; Omary, M. A. *J. Am. Chem. Soc.* **2008**, *130*, 1669.

(13) (a) He, J.; Yin, Y.-G.; Wu, T.; Li, D.; Huang, X.-C. *Chem. Commun.* **2006**, *27*, 2845. (b) Zhang, J.-X.; He, J.; Yin, Y.-G.; Hu, M.-H.; Li, D.; Huang, X.-C. *Inorg. Chem.* **2008**, *47*, 3471. (c) Zhang, J.-P.; Horike, S.; Kitagawa, S. *Angew. Chem., Int. Ed.* **2007**, *46*, 889.

(14) (a) Kishimura, A.; Yamashita, T.; Aida, T. *J. Am. Chem. Soc.* **2005**, *127*, 179. (b) Yang, G.; Raptis, R. G. *Inorg. Chem.* **2003**, *42*, 261. (c) Hayashi, A.; Olmstead, M. M.; Attar, S.; Balch, A. L. *J. Am. Chem. Soc.* **2002**, *124*, 5791.

thermal degradation investigations and phosphorescent properties of these complexes.

Experimental Section

Materials and General Methods. All the solvents and reagents for synthesis were commercially available and used as received. HL was synthesized according to the reported procedure.[15] Infrared spectra were obtained in KBr discs on a Nicolet Avatar 360 FTIR spectrometer in the range of 4000−400 cm^{-1}. Photoluminescence analyses were performed on an Edinburgh FLS55 luminescence spectrometer. Elemental analyses of C, H, and N were determined with a Perkin-Elmer 2400C Elemental analyzer. Thermalgravimetric analyses (TGA) were carried out in a nitrogen stream using a Netzsch TG209F3 equipment at a heating rate of 5 °C/min. Powder X-ray diffraction (PXRD) data were recorded on a Bruker D8 ADVANCE X-ray powder diffractometer (Cu Kα, 1.5418 Å).

Synthesis of $\{CuCl[CuL]_3\}_n$ (1). $CuCl_2 \cdot 2H_2O$ (0.031 g, 0.2 mmol), HL (0.0177 g, 0.1 mmol), *N*,*N*-dimethylformamide (DMF, 7 mL), H_2O (2 mL), and aqueous ammonia (25%, 0.1 mL) were mixed in a 25 mL Teflon-lined stainless steel vessel. The mixture was sealed and heated at 140 °C for 72 h, and then cooled to room temperature at a rate of 5 °C/h. Finally, colorless sheet-like crystals of **1** were obtained in 60% yield (based on HL). Anal. Calcd for $C_{36}H_{42}ClCu_4N_9$ (890.40): C, 48.56; H, 4.75; N, 14.16. Found: C, 48.62; H, 4.68; N, 14.19%. IR (KBr, cm^{-1}): 2965s, 2929w, 2864w, 1606s, 1536s, 1440s, 1374 m, 1214 m, 1051s, 1015w, 833s, 690 m, 570 m.

Synthesis of $\{CuBr[CuL]_3\}_n$ (2). $CuBr_2$ (0.0446 g, 0.2 mmol), HL (0.0177 g, 0.1 mmol), DMF (7 mL), H_2O (2 mL), and aqueous ammonia (25%, 0.1 mL) were mixed in a 25 mL Teflon-lined stainless steel vessel. The mixture was sealed and heated at 140 °C for 72 h and then cooled to room temperature at a rate of 5 °C/h. Finally, yellow prism-like crystals of **2** were obtained in 52% yield (based on HL). Anal. Calcd for $C_{36}H_{42}BrCu_4N_9$ (934.86): C, 46.25; H, 4.53; N, 13.48. Found: C, 46.21; H, 4.48; N, 13.52%. IR (KBr, cm^{-1}): 2962s, 2924w, 2856w, 1609s, 1530s, 1434w, 1370w, 1219w, 1058 m, 1010w, 839 m, 698 m, 571 m.

Synthesis of $\{CuI[CuL]_3\}_n$ (3). CuI (0.0382 g, 0.2 mmol), HL (0.0177 g, 0.1 mmol), aqueous ammonia (25%, 2 mL), and ethanol (7 mL) were mixed in a 25 mL Teflon-lined stainless steel vessel. The mixture was sealed and heated at 160 °C for 44 h, and then cooled to room temperature at a rate of 5 °C/h. Finally, yellow prism-like crystals of **3** were obtained in 30% yield (based on HL). Anal. Calcd for $C_{36}H_{42}Cu_4IN_9$ (981.85): C, 44.04; H, 4.31; N, 12.84. Found: C, 44.01; H, 4.36; N, 12.78%. IR (KBr, cm^{-1}): 2966s, 2924w, 2868w, 1603vs, 1529s, 1431s, 1371 m, 1214 m, 1051s, 1010 m, 834s, 695 m, 570 m.

Synthesis of $\{CuSCN[CuL]_3(MeCN)\}_n$ (4). CuSCN (0.0362 g, 0.3 mmol), HL (0.0177 g, 0.1 mmol), aqueous ammonia (25%, 2 mL), and acetonitrile (7 mL) were mixed in a 25 mL Teflon-lined stainless steel vessel. The mixture was sealed and heated at 140 °C for 72 h, and then cooled to room temperature at a rate of 5 °C/h. Finally, yellow block-like crystals of **4** were obtained in 40% yield (based on HL). Anal. Calcd for $C_{39}H_{45}Cu_4N_{11}S$ (954.08): C, 49.09; H, 4.75; N, 16.15. Found: C, 49.06; H, 4.73; N, 16.18%. IR (KBr, cm^{-1}): 2968s, 2920w, 2130, 2062s 1610vs, 1521s, 1431s, 1375 m, 1218 m, 1052s, 1012 m, 831s, 705 m, 578 m.

Synthesis of $\{Cu_2I_2[CuL]_3\}_n$ (5). CuI (0.0382 g, 0.2 mmol), HL (0.0177 g, 0.1 mmol), acetonitrile (3 mL), ethanol (3 mL), and H_2O (3 mL) were mixed in a 25 mL Teflon-lined stainless steel vessel. The mixture was sealed and heated at 150 °C for 44 h, and then cooled to room temperature at a rate of 5 °C/h. Finally, yellow block-like crystals of **5** were obtained in 33% yield (based on HL). Anal. Calcd for $C_{36}H_{42}Cu_5I_2N_9$ (1172.29): C, 36.88; H, 3.61; N, 10.75. Found: C, 36.83; H, 3.63; N, 10.78%. IR (KBr, cm^{-1}): 2964s, 2920w, 2865w, 1600s, 1525s, 1435s, 1370 m, 1216 m, 1054s, 1017 m, 830s, 698 m, 574 m.

(15) Cui, Q.; Cao, X.-Y.; Tang, L.-F. *Polyhedron* **2005**, *24*, 209.

Table 2. Selected Bond Lengths (Å) and Angles (deg) for Complexes **1**−**5**[a]

Complex **1**

Cu(1)−N(1)	1.864(5)	N(1)−Cu(1)−N(4)	171.1(3)
Cu(1)−N(4)	1.864(6)	N(2)−Cu(2)−N(2)$^{\#1}$	172.6(4)
Cu(2)−N(2)	1.877(5)	N(3)−Cu(3)−N(3)$^{\#2}$	139.1(4)
Cu(3)−N(3)	1.954(5)	N(3)−Cu(3)−Cl(1)	110.18(19)
Cu(3)−Cl(1)	2.317(3)		

Complex **2**

Cu(1)−N(1)	1.862(6)	N(1)−Cu(1)−N(4)	172.6(3)
Cu(1)−N(4)	1.856(6)	N(2)−Cu(2)−N(2)$^{\#5}$	174.1(4)
Cu(2)−N(2)	1.881(6)	N(3)−Cu(3)−N(3)$^{\#5}$	139.1(4)
Cu(3)−N(3)$^{\#3}$	1.970(6)	Br(1)−Cu(3)−Br(1)$^{\#4}$	109.16(7)
Cu(3)−Br(1)	2.505(2)	N(3)$^{\#3}$−Cu(3)−Br(1)$^{\#4}$	98.3(2)
Cu(3)$^{\#4}$−Br(1)	2.603(2)	N(3)$^{\#3}$−Cu(3)−Br(1)	107.54(19)
		Cu(3)−Br(1)−Cu(3)$^{\#4}$	70.84(7)

Complex **3**

Cu(1)−N(1)	1.871(3)	N(1)−Cu(1)−N(8)	177.04(15)
Cu(1)−N(8)	1.874(3)	N(2)−Cu(2)−N(4)	176.29(15)
Cu(2)−N(2)	1.866(3)	N(5)−Cu(3)−N(7)	178.37(15)
Cu(2)−N(4)	1.870(3)	N(6)−Cu(4)−N(9)$^{\#6}$	122.15(14)
Cu(3)−N(5)	1.872(3)	N(6)−Cu(4)−I(1)$^{\#7}$	112.41(10)
Cu(3)−N(7)	1.872(3)	N(9)$^{\#6}$−Cu(4)−I(1)$^{\#7}$	109.86(10)
Cu(4)−N(6)	2.020(3)	N(6)−Cu(4)−I(1)	98.24(10)
Cu(4)−N(9)$^{\#6}$	2.033(3)	N(9)$^{\#6}$−Cu(4)−I(1)	93.54(11)
Cu(4)−I(1)	2.8409(7)	I(1)−Cu(4)−I(1)$^{\#7}$	119.42(2)
Cu(4)−I(1)$^{\#7}$	2.5912(6)	Cu(4)−I(1)−Cu(4)$^{\#7}$	60.58(2)

Complex **4**

Cu(1)−N(1)	1.852(5)	N(1)−Cu(1)−N(8)	176.4(2)
Cu(1)−N(8)	1.862(5)	N(2)−Cu(2)−N(4)	177.0(2)
Cu(2)−N(4)	1.860(5)	N(5)−Cu(3)−N(7)	175.3(3)
Cu(2)−N(2)	1.868(5)	N(9)−Cu(4)−N(10)$^{\#9}$	116.5(2)
Cu(3)−N(5)	1.855(5)	N(6)$^{\#8}$−Cu(4)−N(10)$^{\#9}$	106.9(2)
Cu(3)−N(7)	1.862(5)	N(6)$^{\#8}$−Cu(4)−N(9)	111.0(2)
Cu(4)−N(6)$^{\#8}$	2.070(5)	N(10)$^{\#9}$−Cu(4)−S(1)	104.34(16)
Cu(4)−N(9)	2.047(5)	N(9)−Cu(4)−S(1)	108.95(16)
Cu(4)−N(10)$^{\#9}$	1.994(6)	N(10)−C(37)−S(1)	178.2(6)
Cu(4)−S(1)	2.385(2)	C(37)−S(1)−Cu(4)	99.7(2)

Complex **5**

Cu(1)−N(1)	1.883(5)	N(8)−Cu(1)−N(1)	167.1(3)
Cu(1)−N(8)	1.872(5)	N(2)−Cu(2)−N(4)	172.4(3)
Cu(2)−N(2)	1.850(6)	N(7)−Cu(3)−N(5)	175.9(3)
Cu(2)−N(4)	1.856(5)	N(3)−Cu(4)−I(1)	123.44(18)
Cu(3)−N(5)	1.859(5)	N(3)−Cu(4)−I(2)	119.26(18)
Cu(3)−N(7)	1.857(5)	I(1)−Cu(4)−I(2)	116.11(4)
Cu(4)−N(3)	1.963(5)	N(9)$^{\#11}$−Cu(5)−N(6)$^{\#10}$	101.6(3)
I(1)−Cu(4)	2.5512(11)	N(9)$^{\#11}$−Cu(5)−I(1)	109.97(17)
I(2)−Cu(4)	2.5699(11)	N(6)$^{\#10}$−Cu(5)−I(1)	116.52(19)
Cu(5)−N(6)$^{\#10}$	2.091(6)	N(9)$^{\#11}$−Cu(5)−I(2)	112.84(18)
Cu(5)−N(9)$^{\#11}$	2.024(5)	N(6)$^{\#10}$−Cu(5)−I(2)	105.48(18)
I(1)−Cu(5)	2.6488(11)	Cu(4)−I(1)−Cu(5)	57.33(3)
I(2)−Cu(5)	2.6496(11)	Cu(4)−I(2)−Cu(5)	57.11(3)

[a] Symmetry transformations used to generate equivalent atoms: #1 x, $-y+3/2, z$; #2 $x, -y+1/2, z$; #3 $-x+1/2, y-1/2, -z$; #4 $-x+1, -y, -z$; #5 $x, -y, z$; #6 $x+1, y-1, z$; #7 $-x+2, -y-1, -z$; #8 $x, y-1, z$; #9 $-x, -y, -z+2$; #10 $-x+1/2, y-1/2, -z+1/2$; #11 $x, y-1, z$.

X-ray Crystallography. Data collections were performed on a Bruker-AXS SMART CCD area detector diffractometer at 295(2) K using ω rotation scans with a scan width of 0.3° and Mo Kα radiation (λ = 0.71073 Å). Empirical absorption corrections were carried out utilizing the SADABS routine.[16] The structures were solved by direct methods and refined by full-matrix

(16) *Bruker, SADABS, SMART and SAINT*; Bruker AXS Inc.: Madison, Wisconson, USA, 2002.

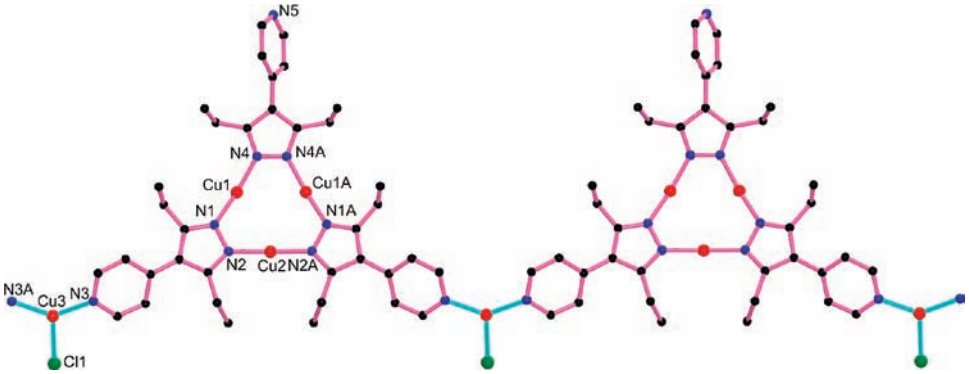

Figure 1. 1D single-strand chain structure in **1**, the N5-pyridyl ring and one ethyl group on N1-pyrazolate ring show 2-fold disorder.

Table 3. Bond Distances (Å) and Bond Angles (deg) of Cu_3 Subunit for Complexes **1**−**5**

	1	**2**	**3**	**4**	**5**
Cu−N	1.864(5)−1.877(5)	1.856(6)−1.881(6)	1.866(3)−1.874(3)	1.852(5)−1.868(5)	1.850(6)−1.883(5)
Cu···Cu (intra)	3.103(1)−3.169(2)	3.094(2)−3.169(2)	3.126(1)−3.194(1)	3.109(1)−3.224(1)	3.100(1)−3.260(1)
Cu···Cu (inter)		5.120(3)	3.311(1)	3.368(1)	
N−Cu−N	171.1(3)−172.6(4)	172.6(3)−174.1(4)	176.29(15)−178.37(15)	175.3(3)−177.0(2)	167.1(3)−175.9(3)

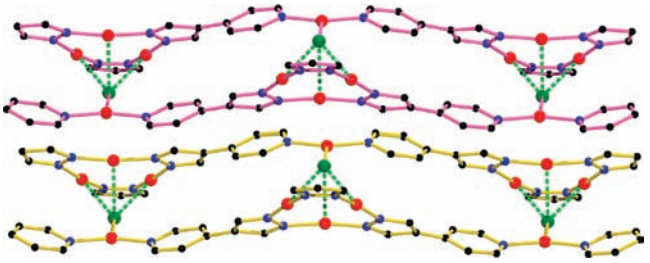

Figure 2. 1D supramolecular double-strand chain in **1**, showing the [**Cu$_3$**]···Cl interactions between adjacent single chains.

least-squares refinements based on F^2.[17] All non-hydrogen atoms were refined with anisotropic thermal parameters, and all hydrogen atoms were included in calculated positions and refined with isotropic thermal parameters riding on those of the parent atoms. The part of ethyl groups on the pyrazolate (in **1** and **3**) and pyridyl rings (in **1** and **2**) are disordered into two discrete positions, which were refined by constraints using the PART command. However, the hydrogen atoms on the disordered ethyl CH_2 groups (C2, **1**; C14, C26, **3**) were not added. Relevant crystallographic data for **1**−**5** are listed in Table 1. Selected bond lengths and angles are given in Table 2.

Results and Discussion

Synthesis. In the present work, HL can be easily deprotonated in the DMF and aqueous ammonia basic solvents, even in a mixed acetonitrile−ethanol−H_2O solvent, moreover, the Cu(II) ions can be in situ reduced to Cu(I) ions during the formation of complexes **1** and **2**, suggesting the strong bonding ability between pyrazolate and monovalent Cu(I) centers. As shown in Scheme 1, the deprotonated L^- ligand is suitable for forming cyclic trinuclear **Cu$_3$** unit with an equal molar ratio of L^- and metal, three vacant pendant pyridyl groups remaining. Therefore, we used a molar ratio of CuX/HL = 2:1−3:1 (X = Cl, Br, I, SCN) to obtain five Cu(I) coordination polymers based on **Cu$_3$** units, possessing planar nine-membered Cu_3N_6 metallocycles with linear two-coordinated Cu(I) as UCMs.

Crystal Structures. Complex **1** crystallizes in the monoclinic space group $P2_1/m$ and has half a **Cu$_3$** unit as well as Cu and Cl atoms with half occupancy per asymmetric unit (Figure 1). The **Cu$_3$** unit exhibits a planar nine-membered Cu_3N_6 metallocycle with the pyrazolate-bridged copper(I) centers featuring a linear coordination geometry (N−Cu−N = 171.1(3)−172.6(4)°) with the Cu−N distances falling in the range of 1.864(5)−1.877(5) Å (Table 2), slightly longer than those in $[Cu(3,5\text{-}(Me)_2pz)]_3$ (Cu−N = 1.845(4)−1.858(4) Å) and $[Cu(3,5\text{-}(CF_3)_2pz)]_3$ (Cu−N = 1.855(2)−1.863(2) Å).[11] The intratrimer Cu···Cu separations are in the range of 3.103(1)−3.169(2) Å (Table 3), shorter than those of structure-related trinuclear copper(I)-pyrazolate complexes (Cu···Cu = 3.20−3.40 Å).[7b,10] Three pyrazolate rings and the Cu_3N_6 plane are nearly coplanar with the dihedral angles of 3.7°, 3.7°, and 9.5°, respectively. The Cu(3) atom shows a trigonal coordination geometry, being surrounded by one terminal Cl atom and two $N_{pyridyl}$ atoms from two different **Cu$_3$** units. Each **Cu$_3$** unit serves as a bitopic linker to bridge two Cu atoms to generate a 1D single-strand chain along the *b*-axis. The Cu3−N3 bond distance of 1.954(5) Å is longer than those in the **Cu$_3$** unit, showing that an increase in the coordination number lengthens the bond distances. Thus, L^- adopts two different coordination fashions: one behaves as a bidentate ligand, leaving one $N_{pyridyl}$ atom uncoordinated, while the other is a tridentate linker.

In **1**, each **Cu$_3$** unit can behave as a π-acid due to containing three UMC Cu atoms, which can easily interact with soft basic Cl atoms through Cu···Cl interactions. The distances between the Cu atoms of **Cu$_3$** unit and Cl atom are 2.782(2), 2.782(2), and 2.809(3) Å, respectively, which are significantly smaller than the sum of the van der Waals radii of Cu and Cl atoms (3.2 Å). Moreover, these strong interactions can also be verified by the deviation of N−Cu−N angles (171.1(3)−172.6(4)°) within the **Cu$_3$** unit from 180°, as well as Cu1 and Cu2 atoms pointing to atom Cl1 due to Cu···Cl interactions. As a result, two neighboring chains connect together to form a supramolecular double-strand chain (Figure 2).

(17) Sheldrick, G. M. *Acta Crystallogr., Sect. A: Found. Crystallogr.* **2008**, *64*, 112.

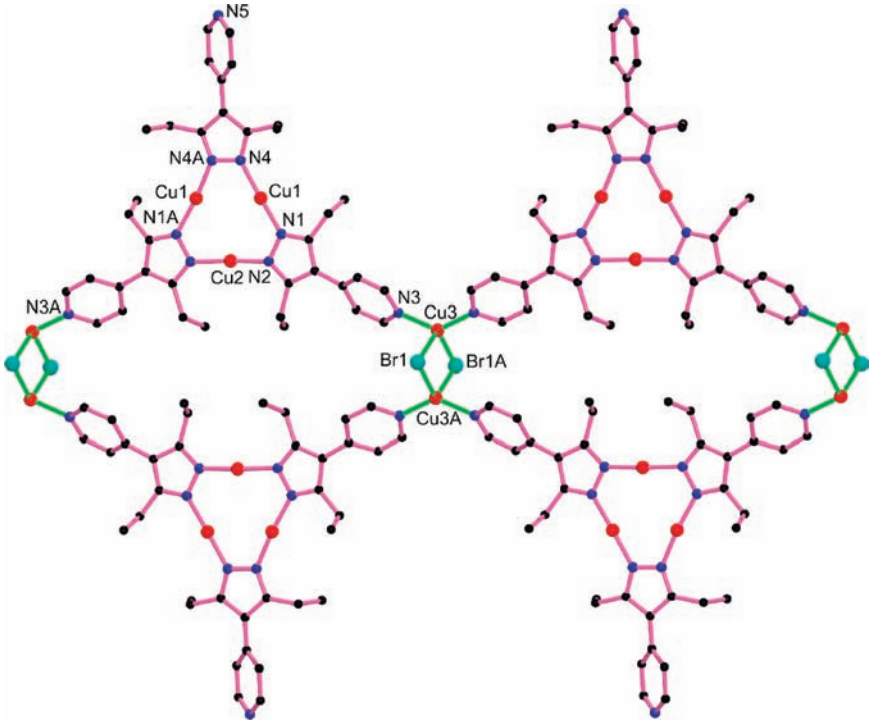

Figure 3. 1D double-strand chain structure in **2**, the N5-pyridyl ring shows 2-fold disorder.

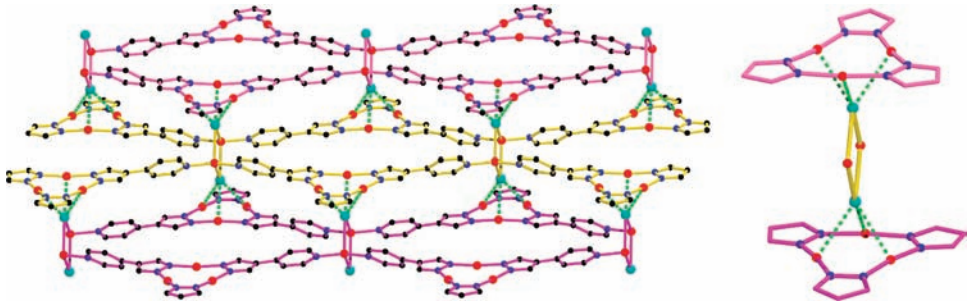

Figure 4. 2D supramolecular structure in **2**, showing the [$\mathbf{Cu_3}$]···Br interactions between adjacent chains (left) and [($\mathbf{Cu_3}$)(Cu_2Br_2)($\mathbf{Cu_3}$)] sandwich substructure (right).

Different from **1**, complex **2** exhibits a double-strand polymer chain. The asymmetric unit of **2** contains half a $\mathbf{Cu_3}$ unit as well as Cu and Br atoms with half occupancy (Figure 3). The solid-state structure of **2** also contains a trinuclear $\mathbf{Cu_3}$ unit with the Cu−N bond distances and N−Cu−N angles being in the range of 1.856(6)−1.881(6) Å and 172.6(3)−174.1(4)°, respectively. The Cu···Cu distances in the $\mathbf{Cu_3}$ unit are 3.094(2)−3.169(2) Å, comparable to those in **1**. Three pyrazolate rings are coplanar with small dihedral angles of 0.5°, 3.5°, and 3.5° in the Cu_3N_6 ring. Two symmetry-related Cu atoms are bridged by a pair of Br atoms to form a rhombic Cu_2Br_2 dimer (Cu···Cu = 2.961(3) Å), which acts as a four-connected junction to bond four $N_{pyridyl}$ atoms from four $\mathbf{Cu_3}$ units, whereas each $\mathbf{Cu_3}$ unit uses two $N_{pyridyl}$ atoms to bridge two Cu_2Br_2 dimers, giving rise to a 1D double-strand chain along the *b*-axis. Thus, each Cu atom in Cu_2Br_2 dimer ligates two $N_{pyridyl}$ atoms and two Br atoms to complete a distorted tetrahedral environment (Cu−N = 1.970(6) Å, Cu−Br = 2.505(2), 2.603(2) Å).

As exhibited in complex **1**, the strong supramolecular π-acid [$\mathbf{Cu_3}$]···Br interactions involved between $\mathbf{Cu_3}$ units and Cu_2Br_2 dimers from the neighboring 1D chains are also observed in **2**, verified by both Cu···Br distances of 2.891(2)−2.929(2) Å and deviation of N−Cu−N angles (172.6(3)−174.1(4)°) from 180°, which lead to a 2D supramolecular layer containing interesting π-acid/Cu_2Br_2 sandwich substructures of [($\mathbf{Cu_3}$)(Cu_2Br_2)($\mathbf{Cu_3}$)] with the Cu_2Br_2 dimer anchored by two $\mathbf{Cu_3}$ units (Figure 4). The adjacent layers are arranged ecliptically along the *c* axis, but with no intertrimer Cu···Cu interactions (Cu···Cu = 5.120(3) Å). The trinuclear coinage-metal pyrazolate complexes show very interesting π-acid properties, as shown in **1** and **2**, however, only sporadic π-acid/base sandwich adducts have been prepared by $[M(3,5\text{-}(Me)_2pz)]_3$ (M = Ag, Au) and electron-rich arene guest molecules, such as benzene, toluene, mesitylene, and naphthalene,[9,11] to the best of our knowledge, π-acid/Cu_2X_2 sandwich complexes have never been reported.

To further research the effects of Cu···X interactions between π-acid $\mathbf{Cu_3}$ units and $(CuX)_n$ motifs on the final structures, CuI and CuSCN were used to replace CuBr, and 1D polymers of **3** and **4** were formed, which, similar to **2**, display double-strand chain structures containing

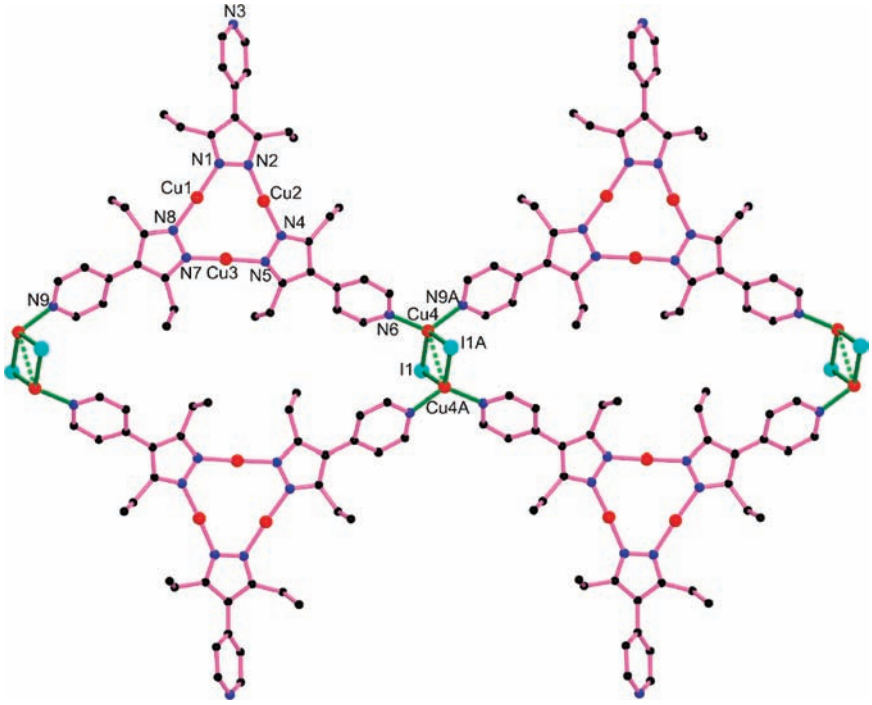

Figure 5. 1D double-strand chain structure in **3**, two different ethyl groups on N4- and N7-pyrazolate rings show 2-fold disorder.

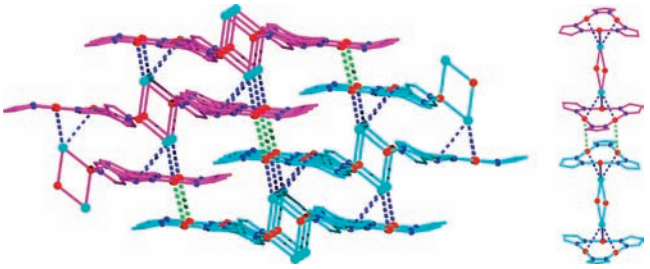

Figure 6. 3D supramolecular framework of **3**, showing the [**Cu$_3$**]···I (dashed blue lines) and intertrimer cuprophilic interactions (dashed green lines) between adjacent chains.

Cu$_3$ units and parallelogram Cu_2I_2 or $Cu_2(SCN)_2$ dimers (Figures 5 and 7). The Cu_3N_6 plane and pyrazolate rings in the **Cu$_3$** units hold coplanarity with the dihedral angles of 4.7°, 10.1°, 13.3° and 6.1°, 6.5°, 6.5° for **3** and **4**, respectively. In the **Cu$_3$** units of **3** and **4**, the Cu···Cu separations are basically equal (3.126(1)−3.194(1) Å, for **3**; 3.109(1)−3.224(1) Å, for **4**), and the Cu−N distances are also close (1.866(3)−1.874(3) Å, for **3**; 1.852(5)−1.868(5) Å, for **4**). It is noted that isostructural $Cu_6L_4X_2$ macrometallocycles exist in **2**−**4**, however, the size of macrometallocycles in **4** is larger than those in **2** and **3**, leading to two guest MeCN molecules being accommodated to stabilize the structure of **4**. Expectedly, in **3** and **4**, weak π-acid/halide or pseudohalide contacts exist between Cu atoms of **Cu$_3$** units and I or S atoms of Cu_2X_2 dimers from the adjacent chains (Cu···I = 3.254(1), 3.321(1), 3.555(1) Å; Cu···S = 3.053(2), 3.167(2), 3.447(2) Å) (Figures S1 and S2, Supporting Information), which lead to 2D supramolecular layers. And as shown in **2**, the [(**Cu$_3$**)(Cu_2X_2)(**Cu$_3$**)] sandwich substructures are generated between one Cu_2I_2 or $Cu_2(SCN)_2$ dimer and two **Cu$_3$** units in **3** and **4**. Interestingly, the neighboring layers in **3** and **4** exhibit eclipsed arrangements along the *c* and *a* axes, respectively, as a result, intertrimer pairs among the adjacent layers are formed through intertrimer Cu···Cu interactions (Figures 6 and 8), at distances of 3.311(1) Å and 3.368(1) Å, respectively. These distances are longer than those in [Cu(3-(CF_3)pz)]$_3$ (3.069 Å),[10] however, much shorter than those in [Cu(3,5-(CF_3)$_2$pz)]$_3$ (3.813(1), 3.987(1) Å)[11] and thus different from **1** and **2**. 3D supramolecular networks are generated in **3** and **4**. In fact, the 1D supramolecular chains can also be formed through π-acid [**Cu$_3$**]···I or S contacts and intertrimer Cu···Cu interactions in **3** and **4** (Figures 6 and 8), respectively, which are unprecedented, even though different types of extended supramolecular [**Cu$_3$**]$_n$ chains or [**Cu$_3$**]$_2$ dimers-of-trimers have been generated through intertrimer Cu···Cu interactions.[7b,10,13]

By reacting CuI with HL under different solvothermal conditions, complex **5** was obtained. **5** is different from the structure of **3** and exhibits a looped double-chain structure containing the tritopic **Cu$_3$** unit and a nonplanar Cu_2I_2 dimer (Figure 9). In **5**, the Cu−N and Cu···Cu distances within the **Cu$_3$** unit are comparable to those in **1**−**4** (Tables 2 and 3), whereas N−Cu−N angles deviate from linearity (167.1(3)−175.9(3)°). The pyrazolate Cu_3N_6 rings are twisted noticeably in **5** with dihedral angles of 10.2°, 13.4°, and 13.6°. In contrast to the parallelogram Cu_2I_2 dimers in **3**, these are nonplanar in **5** and consist of two crystallographically independent Cu(I) centers with different coordination numbers. The Cu(4) atom adopts a trigonal planar geometry to interlink two I atoms and one $N_{pyridyl}$ atom, while the Cu(5) atom is ligated by two I atoms and two $N_{pyridyl}$ atoms from two **Cu$_3$** units to form a distorted tetrahedral coordination. The Cu_2I_2 dimer in **5** exhibits a very short Cu···Cu separation of 2.4960(13) Å, which is much shorter than the sum of the van der Waals radii (2.80 Å) for two adjacent atoms in copper metal and indicates a strong Cu···Cu contact.[18] This dimer can be

(18) Bondi, A. *J. Phys. Chem.* **1964**, *68*, 441.

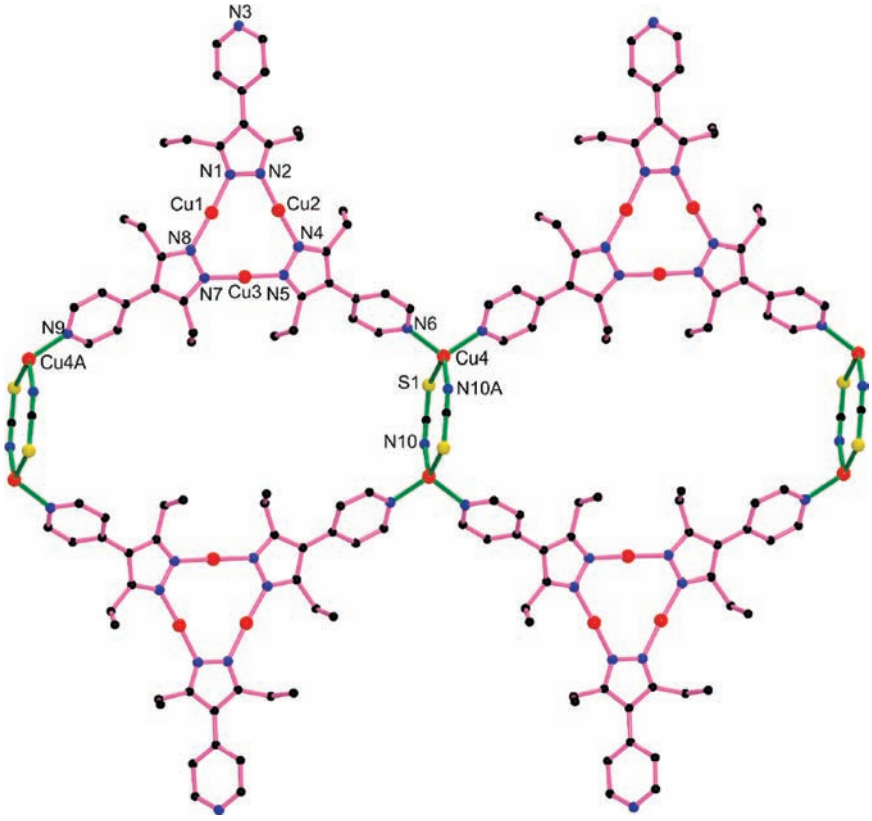

Figure 7. 1D double-strand chain structure in **4**.

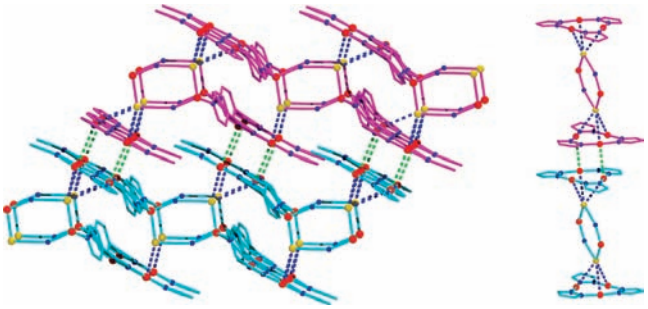

Figure 8. 3D supramolecular framework of **4**, showing the [**Cu$_3$**]···I (dashed blue lines) and intertrimer cuprophilic interactions (dashed green lines) between adjacent chains.

viewed as a three-connected junction due to combining three $N_{pyridyl}$ atoms of three **Cu$_3$** units, which is different from the four-connected role of Cu_2I_2 dimer in **3**. In addition, comparing with two-connected **Cu$_3$** units in **1**−**4**, each **Cu$_3$** unit in **5** acts as a tritopic metalloligand to bridge three Cu atoms of three Cu_2I_2 dimers to generate an interesting 1D looped chain along the *b*-axis. Furthermore, these chains can be stacked by π-acid [**Cu$_3$**]···I interactions between **Cu$_3$** units and Cu_2I_2 dimers from adjacent chains (Cu···I = 3.170(1), 3.208(1), 3.437(1) Å), to give a 2D supramolecular layer parallel to the *ab* plane (Figure 10). Noticeably, the adjacent layers arrange staggeredly along the *c* axis, which leads to a long interlayer Cu···I separation (the closest distance being 4.590(1) Å) between **Cu$_3$** units and Cu_2I_2 dimers, implying no interlayer π-acid [**Cu$_3$**]···I interactions exist, namely, no [(**Cu$_3$**)(Cu_2X_2)(**Cu$_3$**)] sandwich substructure. Therefore, such a supramolecular stacking is similar to that of **1** but different from those 2D/3D supramolecular frameworks of **2**-**4** containing [(**Cu$_3$**)(Cu_2X_2)(**Cu$_3$**)] substructures.

PXRD and Thermal Analysis. The PXRD patterns of **1**−**5** measured at 298 K are in good agreement with their corresponding simulated patterns, confirming phase purities of these samples (Figures S3−S7, Supporting Information). The thermostability of the free ligand HL and **1**−**5** were studied by TGA under nitrogen atmosphere. As shown in Figure 11, the free HL starts to degrade upon heating to 150 °C. For **1**−**3** and **5**, the TGA curves exhibit two-step weight losses in the temperature ranges of 340−440 °C (46.1%) and 440−760 °C (23.4%) for **1**; 365−447 °C (41.8%) and 447−680 °C (21.9%) for **2**; 370−437 °C (40.9%) and 437−755 °C (21.2%) for **3**; 378−450 °C (33.9%) and 450−690 °C (17.1%) for **5**, corresponding to the release of two and one L^- ligands of **Cu$_3$** units, respectively. For **4**, the MeCN molecules (calculated 4.3%, observed 5.1%) were liberated in the temperature range of 70−260 °C, however, the host framework collapses slowly following the removal of the MeCN molecules until ending at 685 °C, which results from the release of solvent molecules from the framework leading to a perturbation of the structure and weakening of coordination bonds, and thus facilitating decomposition of the structure.[19] In comparison with the free HL ligand, the high thermostability of **1**−**5** can be attributed to the strong Cu(I)−pyrazolate coordination bonds and [**Cu$_3$**]···X contacts, which tighten the backbone of the ligand to enhance the resistance to pyrolysis.

(19) de Lill, D. T.; Cahill, C. L. *Chem. Commun.* **2006**, 4946.

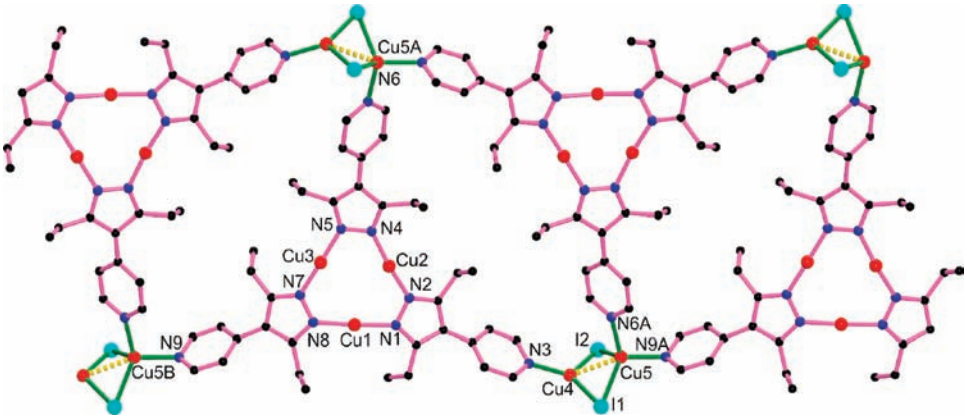

Figure 9. 1D looped double-chain structure in **5**.

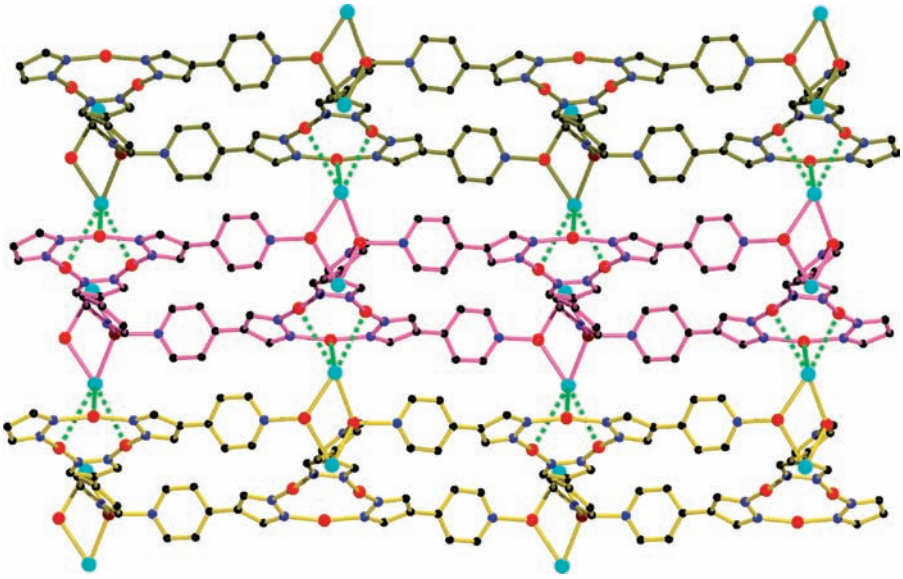

Figure 10. 2D supramolecular framework in **5**, showing the $[Cu_3]\cdots I$ interactions between adjacent chains.

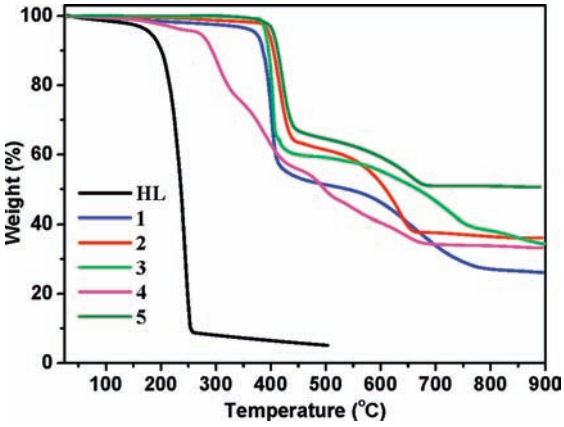

Figure 11. TG curves of HL ligand and **1**−**5**.

Photoluminescence Properties. The solid-state luminescence of HL and complexes **1**−**5** were investigated at room temperature (Figure 12), and the spectral data are summarized in Table 4. All of these complexes exhibit bright luminescence upon exposure to UV radiation due to containing intrinsic luminophor Cu_3 units. The observed lifetimes in the microsecond regime (Table 4) suggest phosphorescence.[10] In the light of the attribution to the emission of cyclic trinuclear copper(I) pyrazolate complexes $[Cu(3,5\text{-}(CF_3)_2pz)]_3$ (550 nm),[7b] $[Cu(3\text{-}(CF_3),5\text{-}(Me)pz)]_3$ (634 nm),[10] $[Cu(3,5\text{-}(Me)_2pz)]_3$ (542 nm),[13a] $[Cu(ppz)]_3$ (564 nm),[13b] and $\{(CuCN)_3[Cu(ppz)]_3\}$ (494 nm)[13b] [ppz = 3,5-dimethyl-4-(4-pyridyl)-pyrazolate], and according to the theoretical calculations of the related cyclic trinuclear copper(I) pyrazolate complexes,[20−22] the emissions of **1**−**5** mainly arise from the metal-centered charge transfer ^{3}[MCCT] excited state for their broad and structureless emission spectra. It is noteworthy that the coordination of halide/pseudohalide atoms in **1**−**5** makes the luminescence stem from multiple origins which can also been reflected by the lifetime data with only fitted by a biexponential decay (Figures S9−S13, Supporting Information). For **1**, besides the metal-centered ^{3}[MCCT] excited state, a mixture of the metal to ligand charge

(20) Gong, F.-B.; Wang, Q.; Chen, J.; Yang, Z.-P.; Liu, M.; Li, S.-Y.; Yang, G.-Q. *Inorg. Chem.* **2010**, *49*, 1658.
(21) Hu, B.; Gahungu, G.; Zhang, J.-P. *J. Phys. Chem. A* **2007**, *111*, 4965.
(22) Grimes, T.; Omary, M. A.; Dias, H. V. R.; Cundari, T. R. *J. Phys. Chem. A* **2006**, *110*, 5823.
(23) Ouellette, W.; Prosvirin, A. V.; Chieffo, V.; Dunbar, K. R.; Hudson, B.; Zubieta, J. *Inorg. Chem.* **2006**, *45*, 9346.

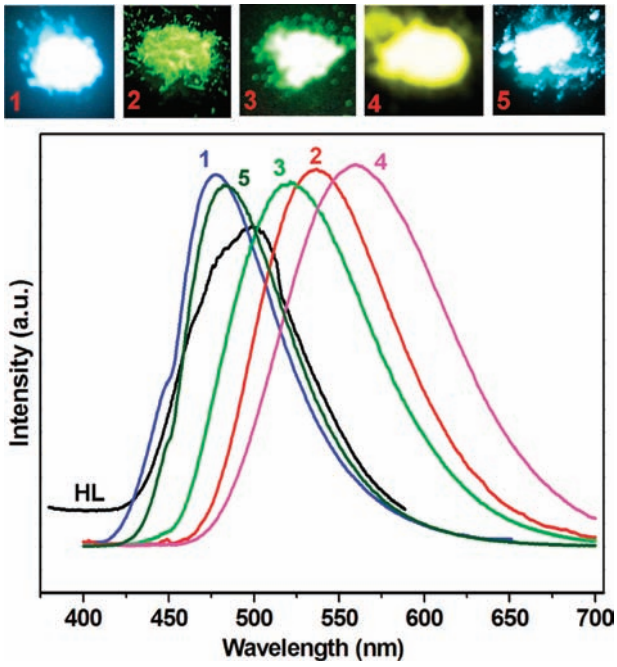

Figure 12. Emission spectra of HL ligand and **1**−**5** in the solid state at room temperature, and snapshots of **1**−**5** under a UV lamp.

Table 4. Emission Data of HL ligand and Complexes **1**−**5**

compd	λ_{ex}/ nm	λ_{max}/ nm	τ/μs	possible origin
HL	315	500	13.14 (ns, 84.54%), 1.85 (ns, 15.46%)	$^3[\pi-\pi^*]$
1	355	476	1.93 (93.12%), 0.46 (6.88%)	^{3}[MCCT], ^{3}[MLCT]
2	397	536	5.41 (80.85%), 1.35 (19.15%)	^{3}[MCCT], ^{3}[XLCT], ^{3}[MLCT]
3	400	525	6.46 (91.21%), 1.94 (8.79%)	^{3}[MCCT], ^{3}[XLCT], ^{3}[MLCT]
4	405	560	6.01 (92.98%), 2.10 (7.02%)	^{3}[MCCT], ^{3}[XLCT], ^{3}[MLCT]
5	397	482	11.06 (88.81%), 4.45 (11.19%)	^{3}[MCCT], ^{3}[XLCT], ^{3}[MLCT]

transfer ^{3}[MLCT] excited state can be assigned.[23,24] It has been observed that $[Cu_2X_2]$-based amine ligand complexes exhibited strong luminescence emissions arising from the MLCT and halide-to-ligand charge transfer (XLCT).[25−29] Therefore, contributions originating from ^{3}[MLCT] and ^{3}[XLCT] excited state should also be involved in the emissions of **2**−**5**. However, the intraligand emission of L^- in **1**−**5** can be excluded on the basis of a short luminescent lifetime of free HL ligand with nanosecond scale (1.85 ns, 13.14 ns, Figure S8, Supporting Information).

The emission maxima for **1** and **5** are quite similar, with only a 6 nm difference, which is in agreement with their similar supramolecular arrangements. However, **2**−**4** exhibit red shifts of emission peaks in contrast to **1** and **5**, which can be attributed to an ample Cu···X interactions in the sandwich substructures of $[(\mathbf{Cu_3})(Cu_2X_2)(\mathbf{Cu_3})]$ because the interactions between coordinatively unsaturated copper(I) centers of π-acid $\mathbf{Cu_3}$ unit and halide/pseudohalide atoms can lead to the low-energy emissions.[3] Additionally, the irradiation of **3** and **4** at the approximate excitation wavelength (400 and 405 nm, respectively) gave rise to different emission bands, with the one of **3** blue-shifted by 35 nm to that of **4**, the shift results from stronger intertrimer Cu···Cu interactions in **3** (3.311(1) Å for **3**; 3.368(1) Å for **4**).[7b,13a] The relatively longer lifetime of **5** (11.06 μs, 4.45 μs), compared with those of **1**−**4**, is ascribed to the more rigid structure since three peripheral pyridyl rings of $\mathbf{Cu_3}$ unit participate in coordination, as well as shorter Cu···Cu separations within Cu_2I_2 dimers in **5**.[24,29,30] Moreover, the disordered conformations of ethyl groups or pyridyl rings of $\mathbf{Cu_3}$ units in **1**−**3** can decrease their emission lifetimes, in particular, **1** exhibits the smallest lifetimes because of the formation of CuCl but not rigid Cu_2Cl_2 units.

Conclusion

In summary, five trimer-based 1D polymers were obtained employing the strategy of facile formation of trinuclear Cu_3N_6 fragment by the usage of pyrazolate derivates and copper(I) centers. The complexes **1**−**5** contain the $\mathbf{Cu_3}$ unit, which either acts as a bidentate metalloligand in **1**−**4** or behaves as a tritopic linker in **5**. Interestingly, each $\mathbf{Cu_3}$ unit can behave as a π-acid because of the coordinatively unsaturated Cu(I) centers, which are involved in π-acid $[\mathbf{Cu_3}]$···halide/pseudohalide interactions in **1**−**5** and lead to the construction of 1D double-stand chains in **1**, 2D supramolecular layers in **2** and **5**, or 3D supramolecular frameworks in **3** and **4** through combining intertrimer Cu···Cu interactions. In particular, the sandwich substructures of $[(\mathbf{Cu_3})(Cu_2X_2)(\mathbf{Cu_3})]$ are formed by π-acid $[\mathbf{Cu_3}]$···halide/pseudohalide contacts in **2**−**4**. All the complexes exhibit bright solid-state phosphorescence because of the contributions of ^{3}[MCCT], ^{3}[XLCT], and ^{3}[MLCT] excited states. Moreover, the emission peaks can be tuned by intermolecular $[\mathbf{Cu_3}]$···halide/pseudohalide contacts, which also enhance the thermostability of the frameworks. In addition, the close resemblance of the $\mathbf{Cu_3}$ units in these complexes shows a stability of the cyclic trinuclear copper(I) pyrazolate configuration, which promises the feasibility of modifying a pyrazole with functional groups or by imposing the $[\mathbf{Cu_3}]$··· anions interactions to construct photoluminescent extended frameworks.

Acknowledgment. This work was supported by the National Natural Science Foundation of China (Grants 20771090 and 21001088), State Key Program of National Natural Science Foundation of China (Grant 20931005), Major Research plan of National Natural Science Foundation of China (Grant 91022004), Specialized Research Found for the Doctoral Program of Higher Education

(24) Zhang, J.-P.; Lin, Y.-Y.; Huang, X.-C.; Chen, X.-M. *J. Am. Chem. Soc*. **2005**, *127*, 5495.
(25) Hu, S.; Zhou, A.-J.; Zhang, Y.-H.; Ding, S.; Tong, M.-L. *Cryst. Growth Des*. **2006**, *6*, 2543.
(26) Chen, Y.; Li, H.-X.; Liu, D.; Liu, L.-L.; Li, N.-Y.; Ye, H.-Y.; Zhang, Y.; Lang, J.-P. *Cryst. Growth Des*. **2008**, *8*, 3810.
(27) Vitale, M.; Ryu, C. K.; Palke, W. E.; Ford, P. C. *Inorg. Chem*. **1994**, *33*, 561.
(28) Araki, H.; Tsuge, K.; Sasaki, Y.; Ishizaka, S.; Kitamura, N. *Inorg. Chem*. **2005**, *44*, 9667.
(29) Zheng, S.-L.; Yang, J.-H.; Yu, X.-L.; Chen, X.-M.; Wong, W.-T. *Inorg. Chem*. **2004**, *43*, 830.
(30) Zheng, S.-L.; Chen, X.-M. *Aust. J. Chem*. **2004**, *57*, 703.

(Grant 20096101110005), China Postdoctoral Scientific Foundation (Grant 20100471627), Natural Science Foundation of Shaanxi Province (Grant 2009JZ001), and Science Research Plan Projects of Shaanxi Provincial Educational Department (Grant 2010JK872).

Supporting Information Available: Crystallographic information files (CIFs), PXRD, additional figures of complexes **3** and **4**, and excitation spectra and luminescence decay of HL ligand and complexes **1**−**5**. This material is available free of charge via the Internet at http://pubs.acs.org.